sphere shift is expected to be proportional to the effective magnetic moment, other things being equal.

The apparent variation of μ_{eff} with temperature was incorporated in the data-fitting process and showed no significant change in the kinetic parameters for FeTMpyP, while for FeTPPS about a 30% change in k_1 was found. The data in the latter case do not define k_1 as well, due mainly to the faster rate of exchange which has less influence on the relaxation of $H_2{}^{17}O$.[11]

The T_{2M} results are interesting in that the lack of field dependence and the negative E_a are not consistent with only the Bloembergen–Morgan model[19] for electron-spin relaxation. We considered other possible relaxation mechanisms including nuclear quadrupole interaction and anisotropic g factors but could not draw any firm conclusions from the data at hand. In general, physically unrealistic parameters were required. This problem does not affect the kinetic conclusions seriously but deserves more study in its own right.

Acknowledgment. This work was supported in part by NSF Grant No. GP-38711X, and acknowledgment is made to the donors of the Petroleum Research Fund, administered by the American Chemical Society, for partial support of this research. We wish to thank Dr. D. B. Bechtold for aid in computing and preliminary studies on the FeTMpyP compound and Dr. E. B. Fleischer for the FeTPPS compound and useful information.

Registry No. Fe^{III}TMpyP, 60489-13-6; Fe^{III}TPPS, 60489-11-4; Fe^{III}TMpyP tosylate, 72331-59-0; H_2O, 7732-18-5.

(19) Bloembergen, N.; Morgan, L. O. *J. Chem. Phys.* **1961**, *34*, 842.

Contribution from the Departments of Chemistry and Biochemistry and Biophysics, Oregon State University, Corvallis, Oregon 97331, Department of Chemistry, University of North Carolina, Chapel Hill, North Carolina 27514, and Department of Chemistry, Stanford University, Stanford, California 94305

Magnetic Properties of a (Tetraphenylporphyrin)iron(III) Thiolate: Fe(TPP)(SC_6H_5)(HSC_6H_5)

S. W. McCANN,[1a] F. V. WELLS,[1a] H. H. WICKMAN,*[1a,b] T. N. SORRELL,[1c] and J. P. COLLMAN*[1d]

Received July 26, 1979

Mössbauer, electron paramagnetic resonance, and magnetic susceptibility data for the title complex are reported for the temperature range 1.4–300 K. The crystalline material prepared by standard methods is magnetically complex. There are at least two magnetic sites, each of which shows temperature-dependent spin-state changes over the interval between 300 K and approximately 100 K. At 300 K, the iron(III) is nearly all in the high-spin $S = {}^5/_2$ state. At low temperature, the iron is in lower spin states or possesses a reduced moment owing to dimerization or cooperative magnetic phenomena. The zero field Mössbauer spectra for sample temperatures below 77 K consist of two major patterns. One of these is a simple quadrupole doublet and the other is a multiline, magnetic relaxation broadened spectrum. The later is sharpened by application of a small polarizing magnetic field and at 4.2 K the Mössbauer parameters are $\Delta E_1 = 1.78 \pm 0.01$, $\delta E_1 = 0.53$ and $\Delta E_2 = 2.82$, $\delta E_2 = 0.38$ mm/s. With increasing temperature ($T > 80$ K), the quadrupole spectra decrease in intensity and are replaced by the same or similar high-spin iron(III) patterns. Conversion temperatures for the two low-temperature species are approximately 250 and 200 K, respectively. In addition to the patterns just described, a low-intensity, sample-dependent high-spin iron(III) pattern is observed; this pattern does not show a significant temperature variation. The susceptibility and EPR data are consistent with the gradual transitions observed in the Mössbauer patterns. The effective magnetic moment of the material decreases slowly from 5.7 μ_B at 300 K to 3.7 μ_B at 20 K, with a sharp decrease occurring below 20 K to a value of 2.8 μ_B at 1.5 K. At room temperature, the major EPR absorption is from high-spin iron(III). This absorption decreases with decreasing temperature and is replaced by a low-spin iron(III) pattern. At helium temperatures, the major absorption is from low-spin iron(III). It is characterized by a g tensor with principal components (2.363, 2.240, 1.965). These values are shown to be incompatible with an isolated $^2T_2$ level and probably reflect a significantly admixed low-spin state. Possible models consistent with these results and with structure data of Strouse and co-workers are discussed. The ligation of the iron in the title complex is similar to that of the active site of cytochrome P-450. Similarities between magnetic properties of the analogue and the enzyme are also considered.

I. Introduction

The subject of this study is an iron(III) porphyrin thiolate that was originally prepared as an analogue for cytochrome P-450.[2] It is well-known that iron in P-450 is bound to at least one sulfur ligand,[3-11] as originally suggested by Mason et al.[3] It is likely that the second axial ligand is nitrogen,[7a,10] although direct structure data to confirm this are not yet available.[11] It is possible that the ligation of iron varies during the complex reaction cycle of P-450. The thiolate discussed in this work is most closely related to the oxidized form of cyt P-450, containing iron(III), as shown in Figure 1. The figure gives the reaction cycle of cyt P-450 from *Pseudomonas putida* (denoted $P\text{-}450_{cam}$) as reported by Gunsalus and co-workers.[4] Several groups have shown that upon substrate (camphor) binding, trivalent iron in $P\text{-}450_{cam}$ is at least 70% converted from the low spin to the high spin form.[5,6] The structural factors involved in this conversion are not understood, and it is desirable to isolate such properties by preparing more easily

(1) (a) Department of Chemistry, Oregon State University. (b) Department of Biochemistry and Biophysics, Oregon State University. (c) University of North Carolina. (d) Stanford University.
(2) Collman, J. P.; Sorrell, T. N.; Hoffman, B. M. *J. Am. Chem. Soc.* **1975**, *97*, 913-4.
(3) Mason, H. S.; North, J. C.; Vanneste, M. *Fed. Proc.* **1965**, *24*, 1172-80.
(4) Gunsalus, I. C.; Meeks, J. R.; Lipscomb, J. D.; Debrunner, P. G; Munck, E. In "Molecular Mechanisms of Oxygen Activation;" Hayaishi, O., Ed.; Academic Press: New York, 1976; pp 559-613.
(5) Sharrock, M.; Debrunner, P. G.; Schulz, C.; Lipscomb, J. D.; Marshall, V.; Gunsalus, I. C. *Biochim. Biophys. Acta* **1976**, *420*, 8-26.
(6) Tsai, R.; Yu, C. A.; Gunsalus, I. C.; Peisach, J.; Blumberg, W.; Orme-Johnson, W. H.; Beinert, H. *Proc. Natl. Acad. Sci. U.S.A.* **1970**, *66*, 1157-63.
(7) (a) Dawson, J. H.; Holm, R. H.; Trudell, J. R.; Barth, G.; Linder, R. E.; Bunnenberg, E.; Djerassi, C.; Tang, S. C. *J. Am. Chem. Soc.* **1976**, *98*, 3707-9. (b) Koch, S.; Tang, S. C.; Holm, R. H.; Frankel, R. B. *J. Am. Chem. Soc.* **1975**, *97*, 914-5.
(8) Tang, S. C.; Koch, S.; Papaefthymiou, G. C.; Foner, S.; Frankel, R. B.; Ibers, J. A.; Holm, R. H. *J. Am. Chem. Soc.* **1976**, *98*, 2414-34.
(9) Koch, S.; Holm, R. H.; Frankel, R. B. *J. Am. Chem. Soc.* **1975**, *97*, 6717-23.
(10) Chevion, M.; Peisach, J.; Blumberg, W. E. *J. Biol. Chem.* **1977**, *252*, 3637-45.
(11) Cramer, S. P.; Dawson, J. H.; Hodgson, K. O.; Hager, L. P. *J. Am. Chem. Soc.* **1978**, *100*, 7282-90.

0020-1669/80/1319-0621$01.00/0

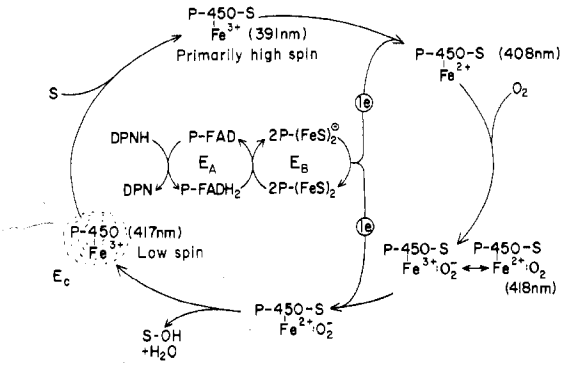

Figure 1. Reaction cycle of soluble cytochrome P-450$_{cam}$ from *Pseudomonas putida*, after Gunsalus et al.[4]

characterized analogue systems.[2,8,12] As shown in this report, however, the analogue structures themselves may turn out to possess unexpectedly complex magnetic properties.

Previous preliminary studies have shown that the thiolate (hereafter denoted SFeS(TPP)) displays thermally driven changes of coordination[13] and spin state.[14] These changes may be related to the effect of substrate binding, as shown in Figure 1. Near room temperature, the iron in SFeS(TPP) is coordinated to the thiolate sulfur ($H_5C_6S^-$). With decreasing temperature, structural changes occur over a broad temperature interval, $100 \lesssim T \lesssim 300$ K. Some of the iron shifts to an in-plane position, and at least partial coordination with thiol sulfur is implicated by the X-ray data. As shown below, this coincides with spectral changes in the Mössbauer data which show a conversion of high-spin iron(III) to lower spin states. The magnetic data also show that the analogue properties are complicated by the presence of more than one magnetic site. There are two major spectral contributions to the Mössbauer patterns; each of these displays spin crossover or similar temperature-dependent features. These properties are also correlated with changes observed in the EPR and susceptibility data. A unique structure–magnetism model to rationalize all of these changes is not yet available. In the discussion, we consider certain possibilities that are consistent with magnetism data.

Where possible, the magnetic properties of SFeS(TPP) are compared with the detailed magnetism data available for particular P-450 enzymes.[4-7a,15-17] It is shown, for example, that one site in SFeS(TPP) corresponds to a low-spin iron(III) species observed in substrated bound P-450$_{cam}$ by Lipscomb and Gunsalus.[17]

Experimental methods are given in section II; the data are described in section III and analyzed in section IV, and a discussion of results is presented in section V.

II. Materials and Methods

A. Materials. The SFeS(TPP) was prepared by the method reported by Collman, Sorrell, and Hoffman.[2] Approximately 0.3 g of (mesotetraphenylporphyrin)iron(III) μ-oxo dimer was dissolved in 70 mL of benzene and stirred for 1 h with 75 mL of 15% H_2SO_4 and 10–15 mL of benzenethiol. The organic layer was separated and 75 mL of 95% ethanol added. The solution was evaporated slowly in a round-bottomed flask under a stream of nitrogen. This yields approximately 0.2 g of Fe(TPP)(SPh)(HSPh) which is in the form of elongated metallic purple crystals. The material is extremely soluble in benzene, giving a dark brown solution. Anal. Calcd for Fe(TPP)(SPh)(HSPh): C, 75.75; H, 4.43; N, 6.31; S, 7.23; Fe, 6.29. Found: C, 75.49; H, 4.47; N, 6.38; S, 7.00; Fe, 6.40.

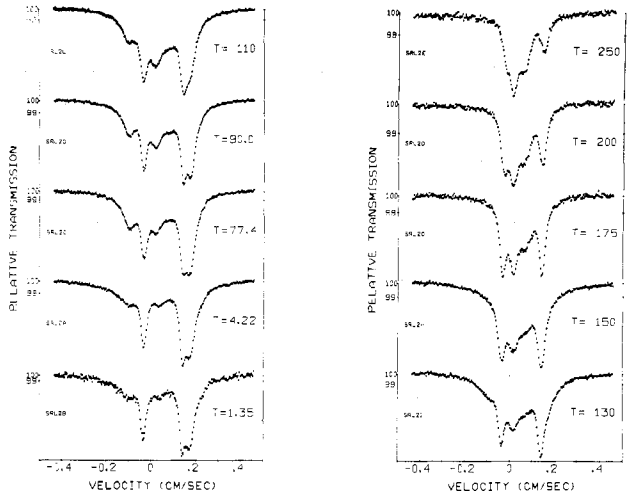

Figure 2. Mössbauer spectra of SFeS(TPP) for the indicated temperatures.

B. Mössbauer Methodology. The spectrometer was of the conventional constant-acceleration type. The source was ^{57}Co diffused in rhodium. All isomer shifts are given relative to natural iron foil at 300 K. The source was mounted on a LVsyn-loudspeaker system driven by a digitally controlled function generator with a standard feedback loop. The radiation was detected by a proportional counter and multichannel analyzer system. SFeS(TPP) is unstable with respect to heavy grinding, so absorbers were lightly milled to minimize texture effects in the absorbers. The sample holder was a two-piece, 2.22-cm diameter Lucite disk with sample area 2 cm^2 and thickness 1.0 mm. It was sealed with silicone grease and stored in liquid nitrogen until use. All workups were carried out in an oxygen- and moister-free environment. The Lucite holder was sandwiched between two 0.025 cm thick low-iron beryllium disks and mounted in a variable temperature probe (heater and sensors) which was used with a Janis vari-temp Dewar. Temperatures above 4 K were monitored and controlled via silicon diode or platinum sensors (accuracy ±0.2 K, stability ±0.15 K). In the liquid-helium region, temperatures were measured with a germanium resistance thermometer. Temperature was varied by standard manometric methods. In some low-temperature runs, a transverse, external polarizing field of 0.2 T was applied to the sample.

C. Magnetic Susceptibility Measurements. Susceptibility data were obtained by the Faraday method with a Cahn RG electrobalance and Houston Instruments 2000 recorder. The magnetic field was provided by a 6-in. diameter Varian electromagnet and field gradient by a George Associates Model 503 Lewis coil. The magnetic field was monitored by using a Hall probe. A Janis Research Co. Model ST helium Dewar was used, employing the same temperature-control methods as the Mössbauer experiments. Samples of 5–10 mg were encapsulated in pure aluminum foil, with the final volume being approximately spherical. The samples were placed in a quartz bucket and suspended by a multifilament nylon thread (120-cm sample-to-balance distance).

D. Electron Paramagnetic Resonance Measurements. The EPR data were obtained with a Varian E-9 spectrometer. Polycrystalline samples were mounted in standard 4-mm o.d. quartz EPR tubes. Temperatures from 90 to 300 K were achieved by using a gas stream heat exchanger attached to a quartz Dewar insert. Temperature was monitored with a platinum-resistance thermometer located in the gas flow approximately 1 cm from the sample. Gas flow was maintained at 10 L min^{-1} to ensure adequate cooling and minimize temperature gradients (less than 0.33 K/cm). The helium-temperature EPR work employed a rectangular cavity (TE_{102} mode) and Gordon type variable coupling slug.[18]

(12) Chang, C. K.; Dolphin, D. *J. Am. Chem. Soc.* **1976**, *98*, 2414–34.
(13) Collman, J. P.; Sorrell, T. N.; Hodgson, K. O.; Kulshrestha, A. K.; Strouse, C. E. *J. Am. Chem. Soc.* **1977**, *99*, 5180–81.
(14) Wickman, H. H.; McCann, S. W.; Sorrell, T. N.; Collman, J. P. *Bull Am. Phys. Soc.* **1977**, *22*, 337.
(15) Herrick, R. C.; Stapleton, H. J. *J. Chem. Phys.* **1976**, *65*, 4783–90.
(16) Champion, P. M.; Münck, E.; Debrunner, P. G.; Moss, T. H.; Lipscomb, J. D.; Gunsalus, I. C. *Biochim. Biophys. Acta* **1975**, *376*, 579–82.
(17) Lipscomb, J. D. Ph.D. Thesis, University of Illinois, 1976 (unpublished).
(18) Gordon, J. P. *Rev. Sci. Instrum.* **1961**, *32*, 658–61.

Table I. Hyperfine Parameters Derived from Mössbauer Spectra for SFeS(TPP)

	LS2		XS1		HS	
temp, K	ΔE_1, mm/s	δE_1, mm/s	ΔE_1, mm/s	δE_1, mm/s	ΔE_1, mm/s	δ, mm/s
4.22	2.82 ± 0.03	0.38 ± 0.03	1.75 ± 0.03	0.53 ± 0.03	*a*	*a*
77	2.74	0.37	1.72	0.54	0.56 ± 0.07	0.44 ± 0.05
130	2.78	0.38	1.78	0.54	0.50	0.38
175	*a*	*a*	1.74	0.55	0.53 ± 0.03	0.40 ± 0.03
250	*a*	*a*	1.69	0.61	0.48	0.34

[a] Not resolved.

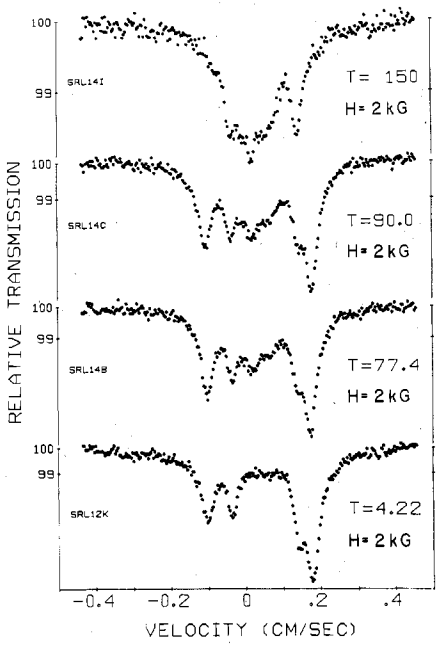

Figure 3. Mössbauer spectra of SFeS(TPP) for the indicated temperatures and magnetic field.

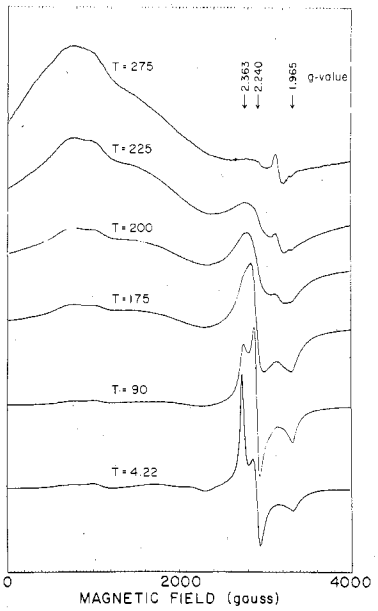

Figure 4. EPR spectra of SFeS(TPP) for the indicated temperatures.

III. Experimental Results

Mössbauer spectra for SFeS(TPP) are shown in Figures 2 and 3. The data are for sample temperatures in the range 1.35–250 K. Above 250 K, the recoil-free fraction of iron decreased rapidly. At most temperatures, the spectra could be described as a superposition of three components: (i) a narrow, asymmetric unresolved quadrupole doublet denoted HS, (ii) a more widely split, resolved doublet denoted XS1, whose line width and line separation varied slightly with temperature, and (iii) a broadened or magnetically split quadrupole pattern denoted LS2. The spin state of the iron(III) in XS1 is not easily deduced from Mössbauer spectra in zero or small ($B \lesssim 0.2$ T) magnetic fields. Arguments given below assign the LS2 spectrum to low-spin iron(III). In the helium temperature region, XS1 and LS2 were the dominant spectral components. Their relative intensities varied slightly with preparation but it is likely that these variations arose from texture effects or particle size distributions as opposed to intrinsic changes in bulk site populations in different materials. In no case was it possible to prepare a sample with only one spectral component present at 4.2 K. Doublet XS1 displayed a slightly temperature-dependent line width (line width increased with increasing temperature). With increasing temperature, both XS1 and LS2 diminished in intensity with concomitant increase in the intensity of peak HS. It appears that both low-temperature states thermally convert to similar or possibly to the same high-spin species, HS1 and HS2.

The spectra given in Figure 3 show the effect of a small (0.2 T) polarizing magnetic field. The field induces a line narrowing which allows a more accurate determination of the quadrupole splittings. The latter are given in Table I. We attempted to determine the temperature dependence of the ratio XS1/HS1 and LS2/HS2. However, it was not possible to obtain a quantitative plot of these ratios. The problem was the similar nature of HS1 and HS2, the unknown recoil-free fraction temperature variations, and the fact that a residual HS pattern was commonly present even in the helium temperature range. Qualitatively, it is clear that in both cases the magnetic or spin transitions occur over a broad temperature interval. In most phenomenological theories of the spin transitions, the transition temperature, T_c, is taken as the point where the high- and low-spin populations are equal. With this convention we estimate the transition temperatures $T_{c1} = 250$ K and $T_{c2} = 200$ K.

The EPR properties of SFeF(TPP) also reflect the presence of high- and low-spin species. Data for several temperatures are given in Figure 4. At 275 K, the pattern consists of a broad peak in the $g \sim 6$–9 region, an ill-defined shoulder near the $g \sim 2$ region, and a sharp resonance near $g = 2$. The sharp $g = 2$ resonance rapidly diminished in intensity with decreasing temperature in the range 300–200 K. The origin of this resonance, observed in all samples, is not understood at present. It may be a sulfur radical cocrystallized with the SFeS(TPP). The remaining spectral features at 275 K are typical of high-spin iron(III). The lines are obviously broadened by spin–spin or other relaxation processes, consistent with the fact that SFeS(TPP) is more magnetically concentrated than cyt P-450; the latter shows much sharper EPR spectra. The broad peaks make g value assignments less accurate in the model compound than in the enzyme. As temperature is decreased, the broad, high-spin iron(III) absorption becomes less intense and is replaced by a nominal, rhombic low-spin iron(III) pattern in the $g \sim 2$ region. The central component of this absorption decreases sharply in intensity between 90 and 4.2 K. This suggests anisotropic line widths in the helium temperature region.

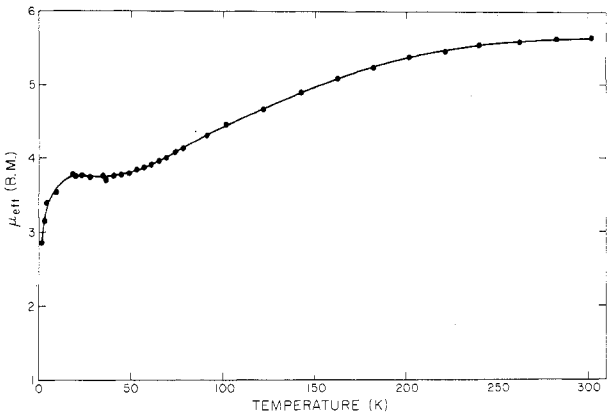

Figure 5. Effective magnetic moment of SFeS(TPP). The magnetic field at all temperatures was 0.54 T.

The low-temperature EPR spectra could not be decomposed into two components, one from XS1 and one from LS2. A single component with g values of 2.363, 2.240, and 1.965 was observed at 4.2 K. We consider in more detail below the possibility that XS1 and LS2 yield the same EPR signal or that one of these species is EPR silent.

The magnetic susceptibility (plotted as effective moment) of polycrystalline SFeS(TPP) is shown in Figure 5. The temperature interval is from 1.4 to 300 K. Those data have been corrected for diamagnetism. Measurements with two orthogonal orientations of the sample were in agreement. At high temperatures μ is near 5.8 μ_B and decreases to a value near 2.8 μ_B at 1.5 K. This behavior is consistent with a gradual conversion of iron(III) from the high- to the low-spin state. Although this is the simplest qualitative interpretation, it should be noted that the data do not rule out more complex effects such as significant splittings of the $^2T_2$ level, admixtures of other configurations, dimerization, or other exchange interactions.

IV. Data Analysis

It is convenient initially to discuss the high- and low-temperature states of iron separately. This is due in part to the fact that distinct spectra from sites or spin states are observed in both Mössbauer and EPR experiments. This means that the spin-state interconversion rate, Ω, is slower than smallest frequency difference, $\Delta\omega$, between spectral line positions. The latter occurs in the Mössbauer spectra and leads to assignment of 10 MHz for Ω.

A. High-Spin Fe(III). This state is observed when ligand field interactions are small compared with exchange and Coulomb energies within the d^5 configuration. The Hund rule $^6A_1$ ground term is then perturbed in complicated fashion by higher order ligand field and spin–orbit interactions which are described by the intraterm spin-Hamiltonian

$$H_{CF} = D(S_z^2 - S(S+1)/3) + E(S_x^2 - S_y^2) \quad (1)$$

with $S = {}^5/_2$. For simplicity, we include only second-rank tensor operators in the spin Hamiltonian. The eigenvalues and eigenfunctions are well-known and can be considered a function of the ratio $\lambda = E/D$.[19-21] The level ordering depends on the sign of D, and it is always possible to use a coordinate system in which $|\lambda| < {}^1/_3$. In iron porphyrins, the parameter D is generally in the range 15–40 cm^{-1}.[22]

When a magnetic field is present, the Zeeman interaction

$$H_M = \beta\vec{H}\cdot g\cdot\vec{S} \quad (2)$$

with $g = 2.0$, must be added to H_{CF}. The Zeeman energies are much smaller than the tetragonal crystal field parameter D, and the EPR spectrum may be described with perturbation g factors for each Kramers doublet. A comparison of polycrystalline EPR spectra with tabulated g values yields an estimate of the rhombicity ratio $\lambda = |E/D|$.

The EPR spectra corresponding to high temperatures ($T \gtrsim 80$ K) are characterized by low-field absorptions with g values near 7.8 and 5.9, a broad resonance near 3.3, and a resonance near $g = 2.0$. These peaks result from a polycrystalline average of resonances from all Kramers doublets in the $^6A_1$ term. In addition, there may be two, slightly different types of high-spin iron centers. However, they are not resolved in either the EPR or ME data and will be assumed identical at this time.

In the temperature range 80–300 K, the Kramers levels are equally populated. It is straightforward to determine whether a value of λ between 0 and ${}^1/_3$ will predict a superposition of spectra corresponding to the data of Figure 4. Inspection of Figure 5 of ref 19 shows that for λ near 0.1, the following three **g** tensors occur: $g_1 = (3.65, 8.03, 1.71)$, $g_2 = (2.28, 2.09, 5.69)$, and $g_3 = (0.07, 0.06, 9.98)$; when $D < 0$, g_1 corresponds to the ground doublet. It is seen that g_1 and g_2 account for the intense peaks near $g = 7.8$ and $g = 5.9$. Likewise, the resonance near $g = 3.3$ is contributed by g_1. Finally, both g_1 and g_2 contribute to the absorption near $g = 2.0$. The agreement is very good, though not exact, since the perturbation treatment has only included second-rank tensor operators.

We now consider the Mössbauer spectra for the high-spin heme species. In the absence of polarizing fields and with fast electronic relaxation, the pattern for trivalent heme iron is a simple quadrupole doublet, often only partially resolved or displaying asymmetry due to relaxation effects.[5,8,23,24] The splitting is described by the ^{57}Fe excited state ($I = {}^3/_2$) nuclear spin Hamiltonian

$$H_Q = \frac{e^2qQ}{4I(2I-1)}[3I_z^2 - I(I+1) + \eta(I_x^2 - I_y^2)] \quad (3)$$

The parameter ΔE, given in Table I, is $(e^2qQ/2)(1 + \eta^2/3)^{1/2}$. That parameter and the isomer shift, δE, are representative of heme iron(III) complexes. The asymmetry in the pattern is attributed to relaxation effects, which can be simulated by model calculations. In the present case, however, accurate values for the crystal field parameters are not known and we postpone discussion of relaxation effects in the high-spin species until this information is available.

The magnetic susceptibility of SFeS(TPP) at high temperature is well approximated by the spin-only magnetism expected for the $S = {}^5/_2$ level with $g = 2.00$. Van Vleck's theorem predicts the value of 5.92 μ_B, which is only slightly higher than the observed value of 5.65 μ_B at 300 K. A somewhat smaller value for the moment is expected, owing to (i) admixtures of $^4T_1$ and $^2T_2$ levels into the $^6A_1$ term and (ii) residual amounts of the low-spin iron(III) species.

B. Component XS1. As shown in Table I, this material has a quadrupole splitting of 1.75 mm/s and an isomer shift of 0.53 mm/s. The latter is somewhat high for iron(III) porphyrins and may suggest an unusual ligand arrangement for the iron(III). We did not observe magnetic hfs for XS1, nor was it possible to assign unambiguously an EPR pattern to

(19) Wickman, H. H.; Klein, M. P.; Shirley, D. A. *J. Chem. Phys.* **1965**, *42*, 2113–7.
(20) Dowsing, R. D.; Gibson, J. F. *J. Chem. Phys.* **1969**, *50*, 294–303.
(21) Blumberg, W. E. In "Magnetic Resonance in Biological Systems"; Ehrenberg, A., Malmström, B. E., Vänngard, T., Eds.; Pergamon Press: London, 1967; pp 119–33.
(22) Brackett, G. C.; Richards, P. L.; Caughy, W. S. *J. Chem. Phys.* **1971**, *54*, 4383–401.
(23) Lang, G. *Q. Rev. Biophys.* **1970**, *3*, 1–60.
(24) Dolphin, D. H.; Sams, J. R.; Tsin, T. B.; Wong, K. L. *J. Am. Chem. Soc.* **1977**, *100*, 1711–8.

Table II. Crystal Field Parameters and Wave Functions for Low-Spin Iron(III) in SFeS(TPP) and P-450$_{cam}$

Crystal Field Parameters

	μ/λ	R/λ	k	g_x	g_y	g_z
LS2	−10.961	4.277	1.583	−2.363 (2.36 ± 0.01	2.240 2.24 ± 0.01	−1.965 1.97 ± 0.01)
P-450	−7.049	3.137	1.146	−2.417 (2.42 ± 0.01	2.249 2.24 ± 0.01	−1.921 1.92 ± 0.01)[a]
P-450[c]				(2.42	2.24	1.97)[b]

Coefficients of the Wave Function $|\psi^{\pm}\rangle = A_i|\pm 1^{\pm}\rangle \pm B_i|\xi^{\mp}\rangle + C_i|\mp 1^{\pm}\rangle$

	i	A_i	B_i	C_i	$(E_i - E_i)/\lambda$
LS2	1	−0.06974	−0.99748	−0.01296	0
	2	−0.77801	0.06252	0.62513	8.849
	3	0.62437	−0.03352	0.78041	13.221
P-450	1	0.1116	0.9935	−0.0229	0
	2	0.79541	−0.1031	−0.5972	5.533
	3	0.5957	−0.0484	0.8017	8.778

[a] Reference 3. [b] References 3 and 16. [c] Substrate bound species.

this site. The susceptibility data show clearly that the bulk moment of XS1 does not correspond to high-spin iron. This leaves lower spin states, $S = {}^1/_2$, $S = {}^3/_2$, or an exchange-coupled ground state for XS1. These possibilities are discussed in section IV.

C. Component LS2. The low-temperature EPR spectra, assumed to correspond to this site, imply that it is low-spin iron(III). In strong octahedral ligand fields, the configuration of iron is $t_{2g}{}^5$ with ground electronic term $^2T_2$. Within this approximation, it is possible to correlate EPR, ME, and susceptibility data in a self-consistent manner. The theory of ligand field and spin–orbit interactions within the $^2T_2$ term has been given by Bleaney and O'Brien[25] and Griffith.[26,27] A useful extension to include hfs was given by Oosterhuis and Lang[28] and Golding.[29] We summarize here the application of these formalisms to LS2. The analysis shows that the theory of an isolated $^2T_2$ level is incomplete in this case. There are, of course, a priori reasons to expect inadequacy of the simple theory. Most important is the neglect, except for introduction of an orbital reduction factor of equivalent multipliers, of admixtures of quartet or sextet levels in the predominantly $^2T_2$ ground state of iron(III).[30,31] It is nevertheless useful to apply the zero-order theory since this allows us to identify points at which quantitative discrepancies arise and which should be removed as more detailed theory and perhaps simpler homologues of SFeS(TPP) become available.

The crystal field and spin–orbit interactions within the $^2T_2$ term are represented by the spin Hamiltonian

$$H_{CF} + H_{SO} = (\mu/9)(3l_z^2 - l(l+1)) + (R/6)(l_x^2 - l_y^2) - \lambda\vec{l}\cdot\vec{S} \quad (4)$$

The parameters μ and R are measures of tetragonal and rhombic ligand field components. The level structure for eq 4 is three Kramers doublets, each of which is characterized by a g tensor. That is, the Zeeman interaction

$$H_M = \beta(k\vec{l} + 2\vec{S})\cdot\vec{H} \quad (5)$$

is treated as a perturbation, and each level is assigned an effective spin $S = {}^1/_2$. The orbital reduction factor, k, is introduced in eq 5. In practice, the experimentally determined g factor for the ground Kramers doublet is used to find the composition of the wave functions for those two states. This information, in turn, is used to compute the tetragonal and rhombic parameters in eq 4. More precisely, the ratios μ/λ and R/λ are determined, and a coordinate system is chosen so that $|R/\mu| \leq {}^2/_3$. Thus one has the option of using tetragonal and rhombic crystal field parameters[32] or g values to parameterize a $^2T_2$ level. The picture is more complex when the orbital reduction factor k is significantly different from unity. To include this possibility, we have carried through an analysis essentially identical with that described by Bohan[33] and earlier workers.[25] The procedure is also described by Herrick and Stapleton[15] and Sharrock et al.[5] in the context of cyt P-450$_{cam}$. Thus we refer the reader elsewhere for details and give only the results of our calculation.[34]

Table III. Parameters Used to Fit Mössbauer Spectra for SFeS(TPP) and P-450$_{cam}$

parameter	P-450[a]	LS2
g_x	1.91	−2.363
g_y	2.26	2.240
g_z	2.45	−1.965
$A_{xx}/g_n\beta_n$, kG	−450	43
$A_{yy}/g_n\beta_n$, kG	102	−71
$A_{zz}/g_n\beta_n$, kG	191	340
$N_{xy}{}^2$	0.96	0.95 ± 0.05
$N_{xz}{}^2$	0.80	0.80 ± 0.1
$N_{yz}{}^2$	0.80	0.80 ± 0.1
ΔE_Q, mm/s	2.85	−2.282
η	−1.80	0.0
$eQV_{zz}/4$, mm/s	0.99	−1.141
δ, mm/s	0.38	0.38
Γ (line width in mm/s)	0.30	0.30
J_q, MHz		45 ± 5
κ	1.14	0.625 ± 0.025

[a] Reference 4.

Table II gives the crystal field parameters and g tensors obtained from a fit to the EPR data for both cyt P-450 and SFeS(TPP). The composition of the ground Kramers doublet, together with covalency factors k and N_{ij}, can be used to compute the hyperfine interactions described by the nuclear spin Hamiltonian

$$H_N = I\cdot A\cdot S + \frac{e^2qQ}{4I(2I-1)}[3I_z^2 - I(I+1) + \eta(I_x^2 - I_y^2)] \quad (6)$$

(25) Bleaney, B.; O'Brien, M. C. M. *Proc. Phys. Soc., London, Sect. B* **1956**, *69*, 1216–30.
(26) Griffith, J. S. "The Theory of Transition Metal Ions"; Cambridge University Press: London, 1961.
(27) Griffith, J. S. *Mol. Phys.* **1971**, *21*, 135–9.
(28) Oosterhuis, W. T.; Lang, G. *Phys. Rev.* **1969**, *178*, 439–56.
(29) Golding, R. M. "Applied Wave Mechanics", D. van Nostrand: New York, 1969.
(30) Harris, G. *Theor. Chim. Acta* **1966**, *5*, 79–97.
(31) Harris, G. *Theor. Chim. Acta* **1968**, *10*, 119–54, 155–80.
(32) Blumberg, W. E.; Peisach, J. In "Probes of Structure and Function of Macromolecules and Membranes", Chance, B., Yonetani, T., Mildvan, A. S., Eds., Academic Press: New York; pp 215–28.
(33) Bohan, T. L. *J. Magn. Reson.* **1977**, *26*, 109–77.
(34) McCann, S. W. Ph.D. Thesis, Oregon State University, 1978 (unpublished).

The resulting hfs is compared with experiment in an iterative fashion. In general, hfs in the presence of an external polarizing yield is required for high accuracy. Lacking this, we used the relaxation broadened spectra for LS2 to derive the parameters of Table III. This involves a relaxation calculation summarized below. Because of the lack of resolution of the spectrum, the parameters of Table III are considered preliminary at this time. No magnetic hfs for XS1 was observed and a similar analysis of this component was not possible. We also note that both lattice and valence contributions to the efg are determined from the crystal field terms and the wave function, respectively.[35] However, the lattice contribution is small and has been neglected in the analysis given here.

Implicit in the foregoing discussion is consideration of electronic relaxation transitions among the ground Kramers levels. The effects of this relaxation upon Mössbauer hfs can be described by several formalisms. The method used here is based on results of Clauser and Blume,[36] Hirst,[37] and Hartmann-Boutron and Spanjaard.[38] The latter method has been applied to low-spin iron(III) by Shenoy and Dunlap,[39] denoted SD. Our method is identical with that of SD, except that we have used anisotropic relaxation rates determined by the electronic **g** tensor for the ground doublet. That is, the relaxation rates between the two Kramers states are given by the expression.

$$W_i = \tfrac{1}{2}g_i^2\beta^2 J_q \qquad i = x, y, z \tag{7}$$

with the g_i as given in Table II, and J_q is the relaxation to spectral density parameter. The spectrum, $I(\omega)$, is computed by Liouville matrix methods as

$$I(\omega) = \mathrm{Re}[\mathrm{F}(\omega)] \tag{8}$$

with

$$\mathrm{F}(\omega) = \sum_{M,M'} (M^{\dagger}_{LM}\tilde{V})(\tilde{\lambda} - i\omega\tilde{1})(\tilde{V}^{-1}M_{LM'}) \tag{9}$$

The diagonal matrix $\tilde{\lambda}$ contains the eigenvalues of the matrix

$$\tilde{U} = \left[(\Gamma - i\omega)\tilde{1} - \frac{i}{\hbar}\tilde{H}_0^{\times} - \tilde{R}\right]^{-1} \tag{10}$$

for the case $\omega = 0$. Likewise, $\tilde{V}$ is the matrix of eigenfunctions of $\tilde{U}(\omega = 0)$. The Liouville matrix $\tilde{H}_0^{\times}$ is defined by $H_M + H_N$. The relaxation matrix $\tilde{R}$ is given in terms of the W_i of eq 7.

$$\langle \mu n \nu m|\hat{R}|\mu' n' \nu' m'\rangle = \delta_{nn'}\delta_{mm'}\Big\{\delta_{\mu\mu'}\delta_{\nu\nu'}\Big[W_z\Big(2\langle\nu|S_z|\nu'\rangle \times \langle\mu'|S_z|\mu\rangle - \frac{1}{2}(W_x + w_y)\Big)\Big] + \Big[\frac{1}{2}(W_x + W_y)\Big][\langle\nu|S_+|\mu'\rangle\langle\mu'|S_-|\mu\rangle + \langle\nu|S_-|\nu'\rangle\langle\mu'|S_+|\mu\rangle] + \Big[\frac{1}{2}(W_x - W_y)\Big][\langle\nu|S_+|\nu'\rangle\langle\mu'|S_+|\mu\rangle + \langle\nu|S_-|\nu'\rangle\langle\mu'|S_-|\mu\rangle]\Big\} \tag{11}$$

The state $|\mu n \nu m\rangle$ is $|S_z^{g} I_z^{g} S_z^{c} I_z^{c}\rangle$.

The relaxation model employs the rate constant J_q as an adjustable parameter at a given temperature. Thus, J_q and the parameters in Tables I and III allow simulation of spectra in Figure 2. In practice, attempts to fit the 4.2 K data showed that the weak, high-spin iron component was relaxation broadened. We chose not to introduce additional parameters to model this component. We show in Figure 6 the result of a fit to the data at 77 K, for two different, early preparations. The value of J_q, 45 MHz, given in Table III, was derived from these data. The computer fits in Figure 6 used the same spectra for each preparation. For simplicity, only the relative intensities for HS, XS1, and LS2 were allowed to vary. Texture or orientation effects could in fact lead to apparent spectral changes for the sites from sample to sample. For this reason, the relative intensities of Figure 6 are only approximate.

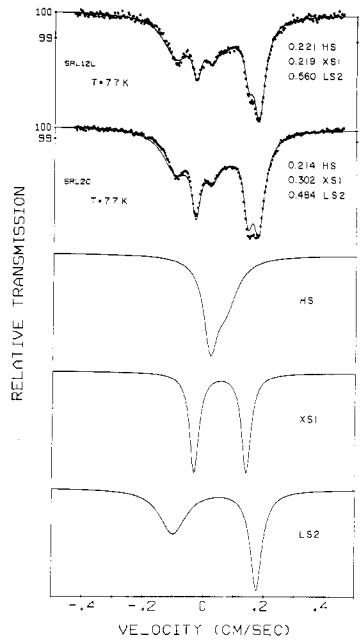

Figure 6. The three components which are summed to simulate the Mössbauer spectra of SFeS(TPP). Parameters for HS andd XS1 are given in Table I. Parameters for LS2 are from Table III. The sample temperature was 77 K.

We now consider the susceptibility data of Figure 5. A complete fit of the data is not possible because of the complex variation of magnetic moment with temperature. As an approximation, we have employed the parameters of Table II and eq 4 to compute the theoretical susceptibility for LS2 and for cyt P-450$_{cam}$. The results of calculations for a value of 400 cm^{-1} for λ show that in the range 5–300 K, the moment increases only about 5% above the value predicted using the g factors of Table II. The low-temperature moment for P-450 is 1.911 μ_B, and for LS2 it is 1.904 μ_B. By contrast the data show a moment of 2.8 μ_B at 1.5 K. At 300 K, the theoretical values are 2.010 and 2.025 μ_B, respectively. It is clear that even in the low-temperature region there is little correspondence between the data and single ion susceptibilities for a $^2T_2$ type term. A second point of interest is the pronounced decrease in susceptibility below about 20 K. This feature is difficult to interpret in terms of paramagnetic susceptibilities and is taken as evidence for exchange interactions in SFeS(TPP).

IV. Discussion

As noted earlier, the preliminary SFeS(TPP) X-ray structure study of Strouse, Collman et al.[13] showed a lattice model which at 113 K consists of a disordered mixture of a six-coordinate complex and a five-coordinate complex. In the latter, the iron is displaced significantly from the heme plane, Figure 7. These data suggested a high-temperature, five-coordinate species in SFeS(TPP) which gradually undergoes a spin and structure crossover to a single, six-coordinate low-temperature form. Often, five-coordinate, out-of-plane heme iron(III) is high spin ($S = {}^5/_2$), and six-coordinate, in-plane iron(III) is

(35) Sharrock, M. Ph.D. Thesis, University of Illinois, 1976 (unpublished).
(36) Clauser, M. J.; Blume, M. *Phys. Rev. B* **1971**, *3*, 583–591.
(37) Hirst, L. L. *J. Phys. Chem. Solids* **1970**, *31*, 655–67.
(38) Hartmann-Boutron, F.; Spanjaard, D. *J. Phys. (Paris)* **1975**, *36*, 301–12.
(39) Shenoy, G. K.; Dunlap, B. D. *Phys. Rev. B* **1976**, *13*, 3709–14.

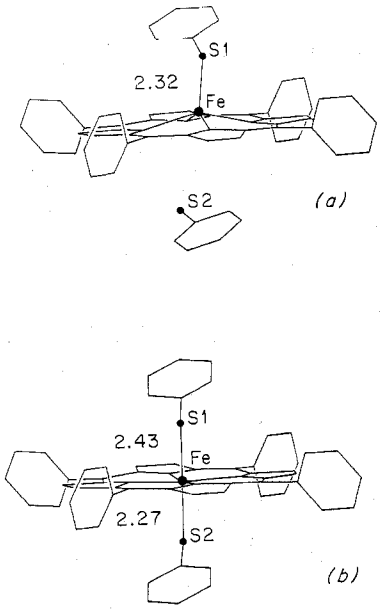

Figure 7. The (a) high- and (b) low-spin forms of SFeS(TPP), after Strouse, Collman et al.[13]

low spin ($S = {}^1/_2$). With this assignment, the X-ray data are qualitatively consistent with magnetism results presented here. However, this study, and particularly the Mössbauer data, shows that SFeS(TPP) contains iron in more than one low-temperature site. The data show clearly that two low-temperature sites are present (XS1 and LS2) together with a small, variable amount of nontransforming material denoted HS3. We also cannot rule out minor contributions from surface states or dislocation sites, if these are different, for example, from the spectral component denoted HS3.

A further complication in structure–magnetism correlations in ferric porphyrin complexes arises because in-plane heme iron(III) need not be in the low-spin state. Recent reports describe interesting examples of in-plane high-spin ferric porphyrin complexes.[40,45,46]

We now consider possible interpretations of the magnetic behavior of SFeS(TPP). Perhaps the simplest explanation of the complex spectra would be crystal allotropism. If true, this would imply one material containing iron(III) in sites with structural and/or magnetic transitions and a second material containing mainly high-spin iron(III), HS3. Since we have been able to prepare samples with very little HS3, we tentatively associate HS3 with an impurity form of SFeS(TPP), possibly formed by interaction with O_2 or H_2O during synthesis or sample preparation. Efforts to minimize such contamination were always made, and the persistence of this component in the face of these efforts is the main indication of a different allotrope. It is also possible that HS3 depends upon crystallite size, surface effects, or loss of lattice solvent occurring during preparation and is not connected with contamination. Strouse and co-workers have not found crystals of SFeS(TPP) with significantly different X-ray parameters. In addition, chemical analyses for all materials have been consistently good with variations much smaller than variations of relative intensities in Mössbauer spectra. This also suggests that if allotropes exist, they do not arise by contamination or by significant loss of benzenethiol from the lattice.

In addition to crystal polymorphism, the possibility must also be considered that SFeS(TPP) contains iron in more than one oxidation state or in intermediate spin states. The presence of divalent iron is unlikely in view of the observed isomer shift parameters which are typical of iron(III) and which are lower than those observed for iron(II). It should be noted that XS1 has a somewhat high isomer shift, 0.53 mm/s, but, interestingly, isomer shifts observed for in-plane high-spin iron(III) heme complexes reported by Reed et al.[40] are also rather high, typically 0.45 mm/s. Possible intermediate spin states of iron(III) are quartet ($S = {}^3/_2$) ground states[7] or states which are highly admixed.[41] We have found no evidence in the EPR patterns for these types of states and there are no precedents for an $S = {}^3/_2$ to $S = {}^1/_2$ spin crossover in heme systems (although this type crossover has been observed in related macrocycles).[43,44] In summary, it is probable that only nominal high- and low-spin forms of iron(III) are present in SFeS(TPP). It is well to emphasize that this conclusion is not unique and others cannot be ruled out completely. For example, we may have $S = {}^3/_2$ sites which antiferromagnetically couple to $S = 0$ ground states which are EPR silent. In view of the already novel nature of the magnetic properties of SFeS(TPP), it is simplest to neglect possibilities which are not implicated directly by the available data or by precedents in other ferric porphyrins.

The picture that emerges at this point is that of a solid with two low-temperature sites (XS1 and LS2) and a third, low population site (HS3) that for simplicity will be assumed to arise from XS1 or LS2 "surface sites". This associates variable site ratios of HS3 and (XS1 + LS2) with crystalline size variations and allows us to view SFeS(TPP) as a solid with two magnetically distinct bulk iron(III) sites, as seen for example by X-ray crystallography. Both XS1 and LS2 display thermally activated changes in coordination or magnetic state. It remains to identify as accurately as possible the nature of these coordination/magnetism changes.

Near room temperature, the susceptibility, Mössbauer, and EPR data all argue conclusively for high-spin iron(III) for both sides: HS1 and HS2. The Mössbauer data do not allow us to say whether the sites are the same or are different. With decreasing temperature, at least part of the high-spin iron(III) converts to low-spin iron(III). This conversion is shown clearly by the EPR spectra which also correlates with changes observed in the Mössbauer data. In terms of the analysis given earlier, this is the conversion of HS2 to LS2. Site 2 is thus occupied by high-spin iron(III) at room temperature and by paramagnetic low-spin iron(III) at helium temperatures.

The second site, denoted HS1 at high temperature and XS1 at low temperatures, is more complex. The main uncertainty is in the nature of the magnetic state at low temperatures. If it is paramagnetic low-spin iron(III), it must have an EPR pattern similar to LS2, since only one prominent low-spin iron(III) EPR pattern is observed. However, the quadrupole splittings of LS2 and XS1 differ, and it is difficult to understand the theoretical basis for this. An alternative explanation would be an EPR silent state for XS1. This could arise from an antiferromagnetic dimer or cluster interaction among high-spin site 1 species leading to an $S = 0$ XS1 spin state below about 50 K, as suggested by the susceptibility data. The antiferromagnetic interaction may or may not depend upon a higher temperature structural transition which, in turn, may or may not involve a spin-state transition. The simplest circumstance would be a structural transition without a spin crossover followed by an antiferromagnetic dimeric interaction

(40) Mashiko, T.; Kastner, M. E.; Spartalian, K.; Scheidt, W. R.; Reed, C. A. *J. Am. Chem. Soc.* **1978**, *100*, 6354–62.
(41) Strouse, C. E., personal communication.
(42) Dolphin, D. H.; Sams, J. R.; Tsin, T. B. *Inorg. Chem.* **1977**, *16*, 711–3.
(43) Hodges, K. D.; Wollman, R. G.; Kessel, S. L.; Hendrickson, D. N.; Van Derveer, D. G.; Barefield, E. K. *J. Am. Chem. Soc.* **1977**, *101*, 906–18.
(44) Earnshaw, A.; King, E. A.; Larkworthy, L. F. *J. Chem. Soc. A* **1969**, 2459–63.
(45) Zobrist, M.; LaMar, G. N. *J. Am. Chem. Soc.* **1978**, *100*, 1944–6.
(46) Spiro, T. G.; Stong, J. D.; Stein, P. *J. Am. Chem. Soc.* **1979**, *1018* 2648–55.

with T_c near 50 K. This would lead to an assignment of XS1 as in-plane, high-spin iron(III), antiferromagnetically coupled and EPR silent at 4.2 K. In this picture, the dominant in-plane structure seen by low-temperature X-ray work would arise from two sites, one involving low-spin iron, the other a possible higher spin state, the simplest being antiferromagnetically coupled $S = {}^5/_2$ ions. Thermal population of excited dimer levels could produce a net susceptibility from site 1 and site 2 that is near the value expected for a system containing only low-spin iron(III).

The model just outlined rationalizes most of the complex magnetic behavior observed in SFeS(TPP). It leaves the nature of the spin-state XS1 somewhat open. Antiferromagnetically coupled $S = {}^5/_2$ is suggested, but $S = {}^1/_2$ or $S = {}^3/_2$ are also possible. The model based on magnetic data is of course unable to assign specific ligand structures for sites 1 and 2. A further point not addressed by the model is the isotropic $g = 2$ signal seen in the EPR spectra above approximately 150 K. If this is indeed a radical signal and it interacts magnetically with an iron(III) site, further complexities arise in the interpretation of the magnetism data. It seems clear at this point that additional structure work together with high magnetic field Mössbauer data and single-crystal EPR studies will be required to achieve a complete understanding of the temperature-dependent magnetic phenomena in SFeS(TPP).

We next consider the low-temperature, low-spin iron(III) LS2 state. Our analysis of the LS2 **g** tensor shows that the ground term is far from a pure $^2T_2$ derived level. The orbital reduction factor is near unity (±15%) when the ground state is predominantly $^2T_2$ and "well behaved". This is the case, for example, in the many low-spin iron(III) complexes which have been analyzed in terms of tetragonal and rhombic crystal field parameters derived from EPR g factors.[10] By contrast, the value of k for LS2 was 1.583, indicating substantial admixtures of quartet levels and the sextet level into the ground term. This implies a crystal field of intermediate strength near the spin crossover region. The origin of admixtures into the ground state is complex and arises via spin–orbit, Coulomb, crystal field, and covalency effects. An analysis of this problem is in progress. However, it is difficult to determine the relative importance of the various contributions on the basis of data for a single homologue.

The present results for LS2 are reminiscent of **g** tensor data observed in substrate bound, oxidized P-450$_{cam}$.[17] Upon substrate binding, P-450$_{cam}$ shows, in addition to a predominant high-spin species ($g = (8, 4, 1.8)$) low-spin forms of two types. One has a **g** tensor similar to that of substrate free P-450 (Table II); the other has $g = (2.42, 2.24, 1.97)$.[16] The latter is similar to the **g** tensor of SFeS(TPP). Lipscomb and Gunsalus have shown that the 1.97 signal is also stabilized at high pH. It is remarkable that in the presence of substrate, P-450 displays EPR properties typical of weak, intermediate, and strong (cubic) ligand fields. These properties further illustrate the sensitivity of the magnetic properties of P-450 to substrate and solvent interactions.[47]

The **g** tensors for the cyt P-450 "1.97 resonance" and SFeS(TPP) are similar but not in exact agreement, (2.42, 2.24, 1.97) vs. (2.37, 2.24, 1.965). This may reflect small differences in coordination in the two cases. If we assume both low-spin forms involve six-coordinate iron(III), we have S_2FeN_4 coordination in SFeS(TPP) and, probably, $SFeN_5$ coordination in cyt P-450.[10,11,45] In the latter case, cysteine and imidazole are implicated by a range of physicochemical measurements. In either case, the predominant influence of sulfur ligation is evident, and we cannot rule out the possibility of S_2FeN_4 ligation in cyt P-450 under some conditions of substrate association.

The comparison of tabulated hyperfine parameters as shown in Table III is only of qualitative significance at this time. On one hand, the accuracy of our analysis, which depends on unresolved hfs is low and, for improvement, must await planned experiments employing an external magnetic field. On the other, we expect a much stronger correlation between the SFeS(TPP) hfs and the $g = 1.97$ low-spin form of P-450. However, the latter have not yet been reported in detail.[4,17] We also note that in Table III, the efg is given as axially symmetric ($\eta = 0$). Although this produced a minimum in our least-squares fit of relaxation spectra, the result is at issue with the low-symmetry environment of the iron. It is expected that an improved determination of this quantity will also result from experiments providing magnetically perturbed spectra.

Acknowledgment. This work was supported in part by National Science Foundation Grant DMR 76-80151. We thank C. E. Strouse for several useful discussions concerning structural and magnetic aspects of SFeS(TPP) and other ferric heme complexes. We thank I. C. Gunsalus, M. Sharrock, and P. G. Debrunner for kindly providing information and discussion of the magnetic properties of cyt P-450$_{cam}$. We also thank G. K. Shenoy and B. D. Dunlap for an early version of the relaxation program used to analyze the SFeS(TPP) Mössbauer data.

Registry No. Fe(TPP)(SC_6H_5)(HSC_6H_5), 54959-14-7; Fe(TPP)(SC_6H_5), 54959-13-6.

(47) Lang, R.; Hoa, H. B.; Debey, P.; Gunsalus, I. C. *Acta Biol. Med. Ger.*, in press.